Microchimica Acta
https://doi.org/10.1007/s00604-017-2588-2

ORIGINAL PAPER

Highly sensitive electrochemical DNA sensor based on the use of three-dimensional nitrogen-doped graphene

Mei Chen[1] · Huilan Su[2] · Li Mao[2] · MingYi Guo[3] · Jiali Tang[3]

Received: 21 August 2017 / Accepted: 23 November 2017

Abstract

This paper describes a voltammetric method for sensitive determination of specific sequences of DNA. The assay is based on three-dimensional nitrogen-doped graphene (3D–NG) which, due to its excellent electrical conductivity, provides a favorable microenvironment to retain the activity of immobilized probe single-stranded DNA and also facilitates electron transfer. The free-standing 3D–NG electrode was characterized by scanning electron microscopy, Raman and X-ray photoelectron spectroscopy, cyclic voltammetry, and electrochemical impedance spectroscopy. Differential pulse voltammetry was applied to monitor DNA hybridization using Methylene Blue as an electrochemical indicator. Under optimal conditions, the peak currents (best measured at 0.28 V vs. Ag/AgCl) increase linearly with the logarithm of the concentrations of ssDNA in the 10 f. to 10 nM concentrations range, with a 3.5 f. detection limit (at a signal/noise ratio of 3). The biosensor exhibits good selectivity for ssDNA and can distinguish even single-base mismatches. The capability of the method was tested with spiked serum samples, and excellent reproducibility and stability is found. This indicates that the strategy is promising for use in clinical applications.

Keywords 3D N-doped graphene · Electrochemical biosensor · DNA detection

Introduction

Deoxyribonucleic acid (DNA) is an essential biomolecule that encodes and regulates the expression of genetic information in living organisms. The determination and quantification of specific DNA sequences is increasingly important for the diagnosis of several genetic diseases, including cancer [1, 2]. Therefore, the highly selective and sensitive detection of specific DNA sequences is a crucial research goal with immense potential in biomedical applications [3, 4]. Many techniques have been developed for DNA detection [5], including fluorescent and chemically modified probes, surface plasmon resonance spectroscopy, and the use of a quartz crystal microbalance [6, 7]. Among these approaches, electrochemical DNA biosensors pose some advantages, including but not limited to high sensitivity, ease of use, low cost, speed, device portability, and the requirement for only small amounts of sample [8–10].

Many functional materials have unique abilities to promote faster electron transfer kinetics, and offer excellent biosensing response characteristics towards a number of biomolecules [11, 12]. Graphene, a two-dimensional (2D) material composed of carbon atoms, is an attractive biosensor material due to its extraordinary electrical, structural, and mechanical properties [13, 14]. Recently, three-dimensional foam-like graphene macrostructures (3D–G) were directly synthesized by chemical vapor deposition (CVD), which comprised a highly electrically conductive network structure that offers increased surface area for biomolecule loading and catalytic reactions [15, 16]. Moreover, the seamlessly interconnected 3D–G networks show

Electronic supplementary material The online version of this article (https://doi.org/10.1007/s00604-017-2588-2) contains supplementary material, which is available to authorized users.

✉ Mei Chen
396762073@qq.com

[1] Department of Biomedical Sciences, Chengdu Medical College, Chengdu, Sichuan 610500, People's Republic of China

[2] School of Public Health, Chengdu Medical College, Chengdu 610500, People's Republic of China

[3] Key Laboratory of Biorheology Science and Technology, Ministry of Education, College of Bioengineering, Chongqing University, Chongqing 400044, People's Republic of China

Published online: 14 December 2017

excellent electrical conductivity, which may improve electron transfer, and therefore may be suitable materials for biosensors [17].

The electrical properties, surface structure, and other intrinsic properties of graphene can be effectively tuned and enhanced by chemical doping with heteroatoms [18]. Among numerous dopants, N-doped graphene (NG) may form stronger interactions with biomaterials, contributing to enhanced biomolecule adsorption capacity [19, 20]. Moreover, compared with pristine graphene, NG shows higher electron activity and better stability in biological and other applications [21, 22]. NG has been used in the oxygen reduction reaction in an alkaline electrolyte, and displayed higher activity and selectivity than graphene [23]. Feng et al. developed a new electrochemical sensor based on NG sheets for the ultrasensitive detection of dopamine [24].

To the best of our knowledge, although 3D–NG has been used in electronic devices and supercapacitors, its applicability to the electrochemical determination of nucleic acid hybridization has not been examined. Here, we use the advantages of a conductive 3D–NG network to develop a new electrochemical DNA biosensor. Chitosan - is a natural polysaccharide derived from the incomplete deacetylation of chitin, and displays remarkable properties such as superior film-forming ability, good adhesion, high water permeability, nontoxicity, and biocompatibility [25, 26]. Considering this, we choose chitosan as a binder to further enhance probe single-stranded DNA (ssDNA) immobilization. In this work, 3D–NG foam was prepared by CVD using nickel foam as a substrate. With the unique architecture and exceptional properties of 3D–NG foam, the biosensor exhibited superior performance for DNA detection, with a low detection limit, a wide detection range, high sensitivity, and good stability in human serum samples. The designed strategy was applied to the ultrasensitive analysis of DNA.

Experimental

Apparatus and materials

Electrochemical measurements were performed on a CHI 600D electrochemical workstation (Shanghai CH Instruments, China). A conventional three-electrode system was used consisting of a modified 3D–G working electrode, a platinum disk auxiliary electrode, and an Ag/AgCl reference electrode. Samples were morphologically characterized using a FEI Nova 400 field-emission scanning electron microscope (FESEM) and a Zeiss LIBRA 200 transmission electron microscope (TEM). The phase composition of the samples was evaluated by X-ray diffraction (XRD) on a Bruker D8 Advance X-ray diffractometer. X-ray photoelectron spectroscopy (XPS) measurements were conducted using a 5300 ESCA instrument (Perkin-Elmer PHI Co., USA). Methylene blue MB and Tris-HCl were purchased from Sigma-Aldrich (St. Louis, MO, USA). Other reagents were purchased from Chongqing Chuan-dong Chemical Co., Ltd. All chemicals were of analytical grade. Deionized (DI) water was produced using a Milli-Q system.

Probe DNA and target DNA were synthesized and purified by Sangon Biological Engineering Tech. Co. Ltd. (Shanghai, China). All oligonucleotide stock solutions were prepared with 0.01 M phosphate buffer (pH 7.4) and stored at 4 °C. Their base sequences were as follows:

Capture probe DNA: 5′- GCTATAATGCGACA GGAGATAGGCT-3′.
Complementary target DNA (CP): 5′-CGAT ATTACGCTGTCCTCTATCCGA-3′.
Single-base mismatched target DNA: 5′-CGAT ATTACGCAGTCCTCTATCCGA-3′
Three-base mismatched target DNA: 5′-CCAT ATAACGCAGTCCTCTATCCGT-3′
Non-complimentary target DNA: 5′-TTGT CCAGGTAGGAGCACAGGATG-3′.

Preparation of 3D N-doped graphene electrodes

The 3D–NG was synthesized by the chemical vapor deposition (CVD) method [27, 28]. Typically, a piece of nickel foam (2 cm × 2 cm, thickness 1.0 mm) was employed as the growth template and put into a quartz tube under H_2 (20 sccm) and Ar (200 sccm). Ethylenediamine (0.25 mL) was the precursor and the reaction temperature was raised from room temperature to 900 °C at a heating rate of 10 °C. min^{-1}. The reaction was allowed to proceed for 30 min. Then, after cooling down to room temperature, the nickel foam was removed to obtain the final product as the follow procedure. The 3D–NG/Ni foam was drop-coated with a PMMA solution, and then dried for 10 min at 150 °C. Thus, a thin PMMA film that prevents the destruction of graphene structure upon the removal of the nickel template was formed on the 3D–NG surface. Then, nickel was removed by immersing the sample in HCl

(3 M) solution at 80 °C for 5 h. Finally, the freestanding 3D–NG was obtained by dissolving the PMMA protective layer in hot acetone. After washing with DI water, the freestanding 3D–NG was fabricated as an electrochemical electrode.

Fabrication of the DNA electrochemical biosensor

0.25 g Chitosan was added to 1% acetic acid to obtain a 0.5 wt% chitosan solution. Then 3D–NG was immersed into the solution and ultrasonicated for 2 h to fabricate the 3D–NG chitosan composite. After that, the sample was washed with DI water to clean the acetic acid on the surface. After drying at room temperature, 5 μL of ssDNA (1×10^{-6} M) solution was drop-cast to cover the modified electrode and incubated for 1.5 h at 25 °C. The electrode modified with probe DNA was then obtained (Fig. 1).

Hybridization with target ssDNA and electrochemical measurements

Hybridization was performed by immersing the probe DNA modified electrode into buffer (pH 7.4) containing various concentrations of target DNA at 30 °C for 50 min. The hybridized electrode was rinsed with buffer to remove any nonspecifically adsorbed DNA and was incubated in a 20 μM Methylene Blue solution (containing 20 mM NaCl) for 20 min and then washed by sodium dodecyl sulfate (SDS) solution. Cyclic voltammetric (CV) were carried out with the scan rate of 100 mV/s. Electrochemical impedance spectroscopy (EIS) investigation was performed with the frequencies ranging from 10^4 to 10^{-1} Hz. Finally, the electrochemical response was measured by differential pulse voltammetry (DPV) in 0.1 M buffer (pH 7.5) using a scanning from −0.5 V to 0 V (modulation time: 50 ms, interval time: 0.5 s, step potential: 5 mV, modulation amplitude: 50 mV).

Results and discussion

Characterization of the 3D–NG-based biosensor

The morphology was characterized by using SEM. The well-defined, foam-like, porous structure of 3D–NG is shown in Fig. 2a. The pore diameter ranged from 200 to 600 μm. Fig. 2b–e exhibits the porous structure of the

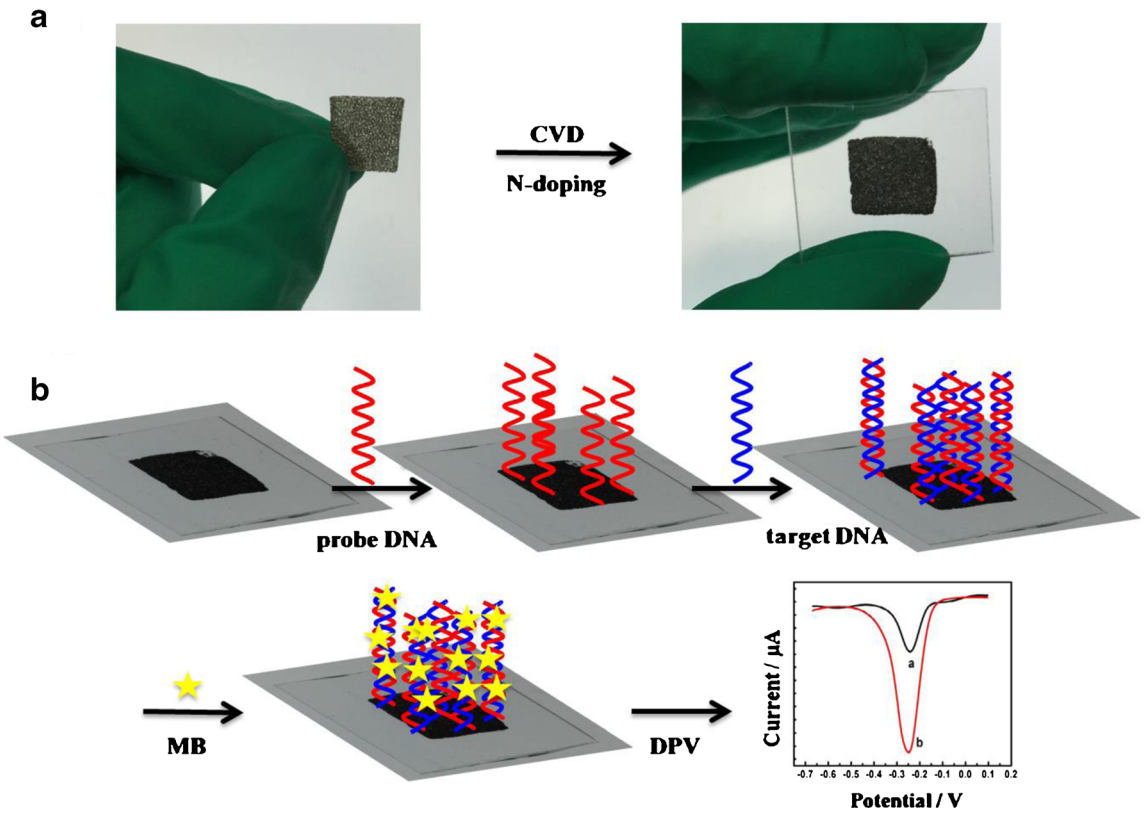

Fig. 1 **a** Fabrication process for 3D–NG. **b** Fabrication and detection process of the DNA biosensor

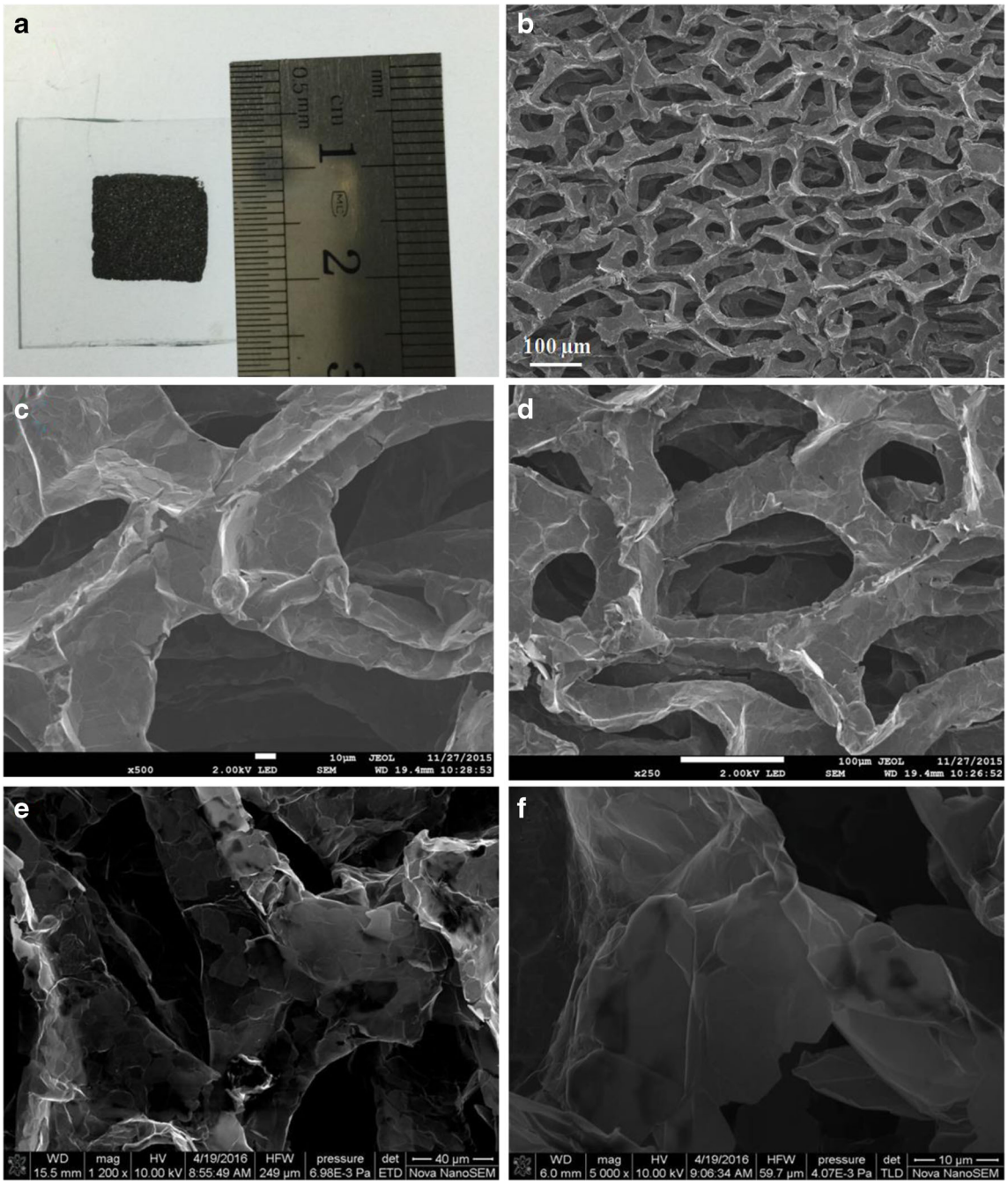

Fig. 2 **a** Photographs of graphene grown on nickel foam. **b-f** SEM images of the CVD-grown 3D–NG with different magnification

interconnected 3D scaffold. High-magnification SEM demonstrated wrinkles on the 3D–NG surface (Fig. 2f), which are typical features of CVD-grown graphene, and were generated by differential thermal expansion during the growth process.

The Raman spectra of 3D graphene and 3D–NG foam obtained at different positions are shown in Fig. 3a. The relatively weak 2D bonds indicate the presence of graphene sheets with few layers. For 3D–G, there was no obvious D band which indicates the absence of significant defects. When nitrogen atoms were doped into the graphene foam, the D band was observed at 1355 cm^{-1}. The D band is usually related to a series of defects, including bonding disorders and vacancies in the graphene lattice induced by nitrogen doping.

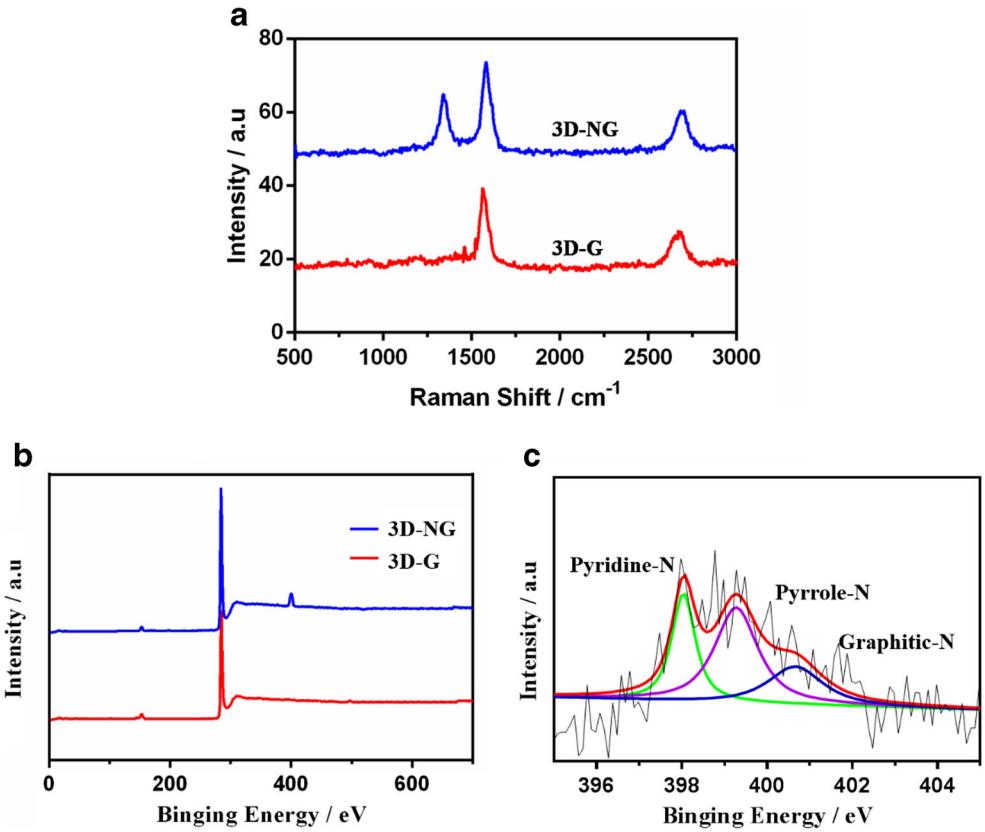

Fig. 3 **a** Raman spectra of 3D–NG and 3D–G. XPS spectra of (**b**) survey scan of 3D–NG and 3D–G. **c** N 1 s narrow scan of 3D-NG

Survey scans of 3D–NG and 3D–G, and N 1 s narrow scan XPS spectra of 3D–NG are shown in Fig. 3b. A predominantly narrow C 1 s peak at ~285 eV was obtained with both 3D–NG and 3D–G, while the N 1 s peak at ~400 eV was present only with 3D–NG. The corresponding element contents in 3D–NG are 97.29% and 2.71% for C 1 s and N 1 s, respectively [29]. The 3D–NG contained no Ni, indicating that its successful removal by acid treatment. The high-resolution XPS N 1 s spectrum shown in Fig. 3c reveals the presence of five types of nitrogen atoms within the graphene structure, including pyridinic N (398.3 eV), pyrrolic N (400.4 eV), graphitic N (401.3 eV), N-oxide (403.3 eV), and N_2 (405.5 eV).

Electrochemical properties of the prepared biosensor

CV was used to test the performance of the modified electrode. Fig. 4a displays several CV curves corresponding to different graphene-based electrodes, including (a) conventional 2D graphene, (b) 3D–G, and (c) 3D–NG. Curve c shows the highest current value, suggesting that 3D–NG has the best electrochemical activity. The results indicate that the 3D structure and the doped-N atoms of 3D–NG enhance the electron transfer rate and improve the electrocatalytic activity. The N-doping along with the high specific surface area of the 3D porous structure provided an abundance of adsorption sites for probe ssDNA loading. When ssDNA was successfully adsorbed on to the electrode, there was an obvious decrease in the current (curve d), suggesting efficient immobilization. After hybridization with target DNA, the peak current of the modified electrode further decreased (curve e). The reason for the decrease is that the movement of $[Fe(CN)_6]^{4-/3-}$ towards the electrode surface is hindered by the presence of DNA molecules.

Electrochemical impedance spectroscopy (EIS) was also used to characterize the different electrodes (Fig. 4b). For EIS, $[Fe(CN)_6]^{4-/3-}$ was utilized as the redox probe and the semicircle diameter was equal to the electron-transfer resistance. The data were fit with an equivalent circuit (inset in Fig. 4b). EIS results were also in good agreement with the CV responses of $[Fe(CN)_6]^{4-/3-}$ on the different modified electrodes, indicating the successful fabrication of the DNA biosensor.

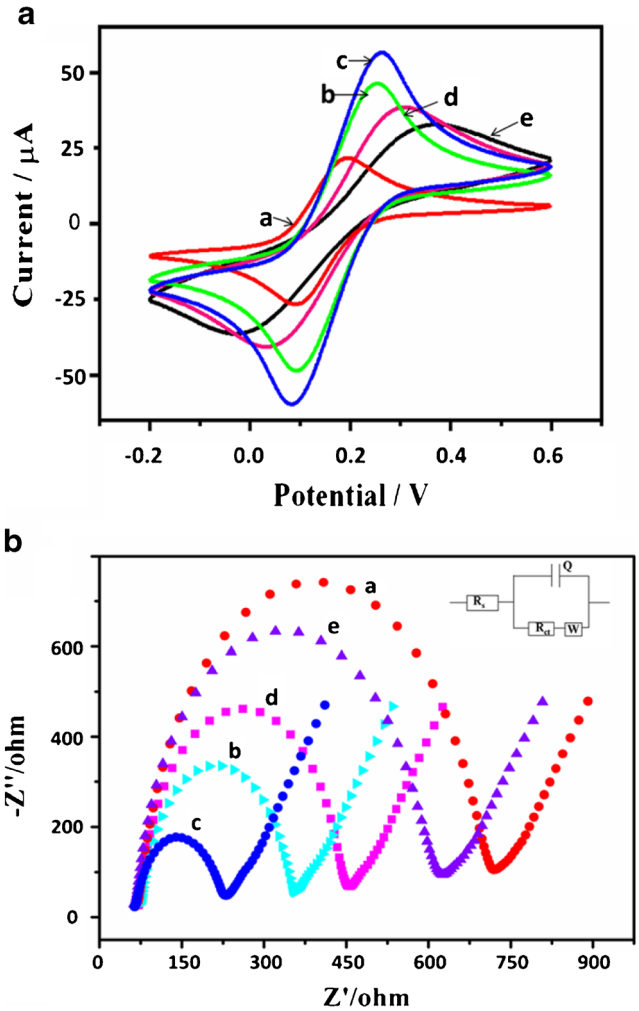

Fig. 4 **a** CV of different modified electrodes in 1.0 mM $Fe(CN)_6^{3-/4-}$ containing 0.1 M KCl solution. 2D–G (*a*), 3D–G (*b*), 3D–NG (*c*), ssDNA/3D–NG (*d*), dsDNA/3D–NG (*e*). **b** EIS characteristics of different modified electrodes in 1.0 mM $Fe(CN)_6^{3-/4-}$ containing 0.1 M KCl solution. 2D–G (*a*), 3D–G (*b*), 3D–NG (*c*), ssDNA/3D–NG (*d*), dsDNA/3D–NG (*e*)

Optimization of the experimental conditions

The following parameters were optimized: (A) pH value; (B) hybridization temperature and (C) hybridization reaction time. Respective data and Figures are given in the Electronic Supporting Material. The following experimental conditions were found to give best results: (A) A pH value of 7.5; (B) hybridization temperature of 30 °C; (C) hybridization temperature of 50 min.

Target DNA sensing

Differential pulse voltammetry is a sensitive electrochemical technique that is widely applied for analytical purposes. The sensitivity of the 3D–NG DNA biosensor was investigated under optimal conditions by varying the target DNA

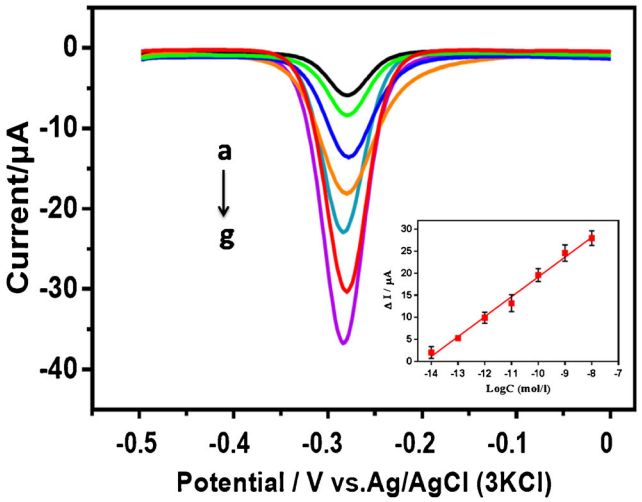

Fig. 5 DPV curves after hybridization with 0 M, 1.0×10^{-14} M, 1.0×10^{-13} M, 1.0×10^{-12} M, 1.0×10^{-11} M, 1.0×10^{-10} M, 1.0×10^{-9} M, 1.0×10^{-8} M target ssDNA (curves a-g, respectively), Inset: plot of peak current vs. log of the concentration of target ssDNA

sequence. Freestanding ssDNA/3D–NG on the ITO was used as the work electrode. As displayed in Fig. 5, the electrochemical response was very sensitive to changes in the target DNA concentration, rising with increased DNA concentration. The peak currents were logarithmically related to the target DNA concentration from 1.0×10^{-14}–1.0×10^{-8} M and the corresponding regression equation was $\Delta I\ (\mu A) = 64.23 + 4.506 \times \lg c\ (M)$, with a correlation coefficient of 0.9927. The limit of detection was estimated to be 2.38×10^{-15} M ($n = 3$). The sensor was compared to other electrochemical DNA biosensors. Table 1 shows that it displays excellent performance owing to its 3D porous structure, which provides a large surface area with excellent electrical conductivity.

Specificity, reproducibility, and stability of the DNA biosensor

The ability of the biosensor to selectively detect DNA of a specific sequence is extremely important. The specificity of the proposed biosensor was investigated by exposing it to equal concentrations of four DNA sequences: a perfect complementary target sequence (TD), a one-base mismatch sequence (1TD), a three-base mismatch sequence (3TD), and a non-complementary sequence (NC; Fig. 6a). As anticipated, the highest peak current increment was observed after hybridization with the TD. However, when hybridized with the NC, the current changes were comparable to the blank. In addition, the peak current was higher with a one-base mismatch compared with three, suggesting that the sensor can distinguish between these sequences. These results indicate the advantageous selectivity of the sensor.

Moreover, the reproducibility of the biosensor was confirmed by preparing five DNA biosensors and using

Table 1 Comparison of linear ranges and detection limits of the different electrochemical DNA sensors

Modified material and electrode	Detection technique	Linear range (M)	Detection limit (M)	References
Ag/CCTS/O_2/Si	DPV	100 f - 10 nM	17 nM	[30]
MPA/GO-PAMAM/Au/AuE	DPV	1.0 pM - 1.0 μM	1.0 pM	[31]
MNAzyme	DPV	100 pM - 0.25 μM	79 pM	[32]
Ph-NH_2/GO/GCE	EIS	1.0 pM - 1.0 μM	11 pM	[33]
Au NPs/TB–GO	DPV	1.0×10^{-11} -1.0×10^{-9}	2.9 pM	[34]
CdS-labeled blocker DNA	DPV	5.0 pM - 1.0 nM	1.2 pM	[35]
Au-rGO-PANI	DPV	0.1 pM - 10 nM	50 fM	[36]
3D–NG	DPV	1.0×10^{-14} -1.0×10^{-7}	3.5 fM	This work

them to detect the TD at 1.0×10^{-10} M. The relative standard deviation (RSD) of the measurements for the five electrodes was 4.3%, which is very low and demonstrates the high reproducibility of DNA detection. These results might be attributed to the excellent conductivity and good construction of 3D–NG. Similarly, the stability of the biosensor was investigated over the course of one week (one measurement per day) using five biosensors independently. The values obtained showed no distinct changes (Fig. 6b), which indicated that the biosensor had sufficient stability for the continued detection of the TD.

Detection of DNA in human plasma samples

The biosensor was tested in human blood serum samples under optimal experimental conditions, and the determination of target DNA was performed by the standard addition method. Blood samples were diluted 100× in 0.10 M phosphate-buffered saline. As shown in Table 2, the biosensors displayed good recovery values (94–103.7%) with an RSD of 1.83–3.08%. These results indicate that our proposed biosensor has great potential in clinical applications.

Conclusions

In this study, an innovative and simple electrochemical DNA biosensor was successfully fabricated from 3D–NG. Because of its high electron transfer efficiency and large surface area for probe ssDNA loading and catalytic reactions, the 3D NG-based biosensor displayed extremely high sensitivity, good selectivity, and repeatability. Under optimum conditions, the biosensor had a detection limit of 2.38×10^{-15} M and a linear range (1.0×10^{-14}–1.0×10^{-8} M), successfully discriminates the target DNA from even single-base mismatches, and displayed good performance in human blood serum samples. Importantly, this electrochemical DNA biosensor can be conveniently applied to other nucleic acids by changing the corresponding DNA sequences. But this biosensor is Methylene blue needed; further action is exploit no labeling process or external indicators. Thus more research is needed to generate reliable, robust, sensitive microchip technology for rapid and automated nucleic acid analysis in real samples, we believe that our present work will result in novel biosensors for diagnostic use against difficult to cure diseases such as cancer. Future efforts in our laboratory will be directed toward this goal.

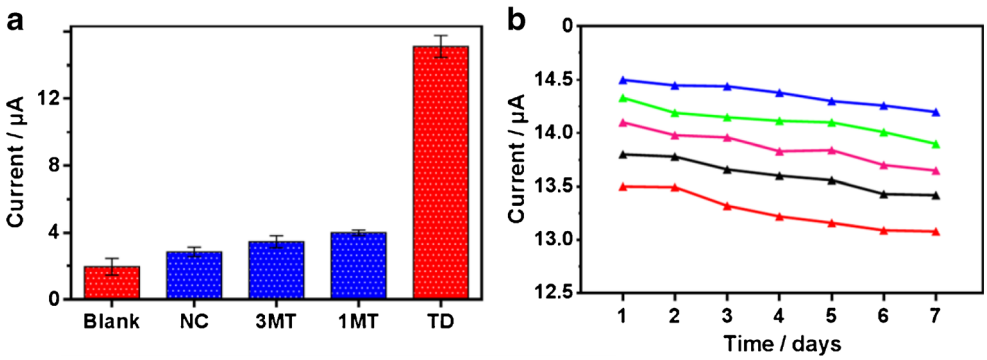

Fig. 6 **a** Comparison of DPV responses of the blank and the four different types of DNA sequences. (single-base mismatch target, 1MT; three-base mismatch target, 3MT; noncomplementary sequence, NC). **b** Signal intensities of the five biosensors (a–e) were obtained within 1 week

Table 2 Recoveries from spiked human plasma samples

Samples	Addd(nM)	Biosensing method (nM)	Recovery (%)	RSD (%)
1	0.5	0.51	102	1.83
2	2.0	1.88	94	3.08
3	4.0	3.91	97.75	2.0
4	6.0	5.93	98.83	2.9
5	8.0	7.98	99.75	1.99
6	10.0	10.37	103.7	2.02

[a] Each value is the mean of five replicate experiments

Acknowledgements The authors would like to acknowledge the financial support from "the National Natural Science Foundation of China (N.O. 81401757 and N.O.81601859)", "Scientific Research Fund of Sichuan Provincial Education Department (No. 11ZA205)" and sharing fund of Chongqing university's large equipment.

Compliance with ethical standards The author(s) declare that they have no competing interests.

References

1. Ling H, Wu Q, Guo J, Xu L, Que Y (2015) Comprehensive Selection of Reference Genes for Gene Expression Normalization in Sugarcane by Real Time Quantitative RT-PCR. PLoS One 10(3): e97469
2. Li H, Cao YX, He XX, Fu SH, Lyu Z, He Y, Gao XY, Liang GD, Wang HY (2015) Real-time RT-PCR Assay for the detection of Tahyna Virus. Biomed Environ Sci 28(5):374–377
3. Li W, Liu XJ, Hou T, Li HY, Li F (2015) Ultrasensitive homogeneous electrochemical strategy for DNA methyltransferase activity assay based on autonomous exonuclease III-assisted isothermal cycling signal amplification. Biosens Bioelectron 70:304–309
4. Holdenrieder S, von Pawel J, Dankelmann E, Duell T, Faderl B, Markus A, Siakavara M, Wagner H, Feldmann K, Hoffmann H, Raith H, Nagel D, Stieber P (2009) Nucleosomes and CYFRA 21-1 indicate tumor response after one cycle of chemotherapy in recurrent non-small cell lung cancer. Lung Cancer 63(1):128–135
5. Kersting S, Rausch V, Bier FF, von Nickisch-Rosenegk M (2014) Multiplex isothermal solid-phase recombinase polymerase amplification for the specific and fast DNA-based detection of three bacterial pathogens. Mikrochimica Acta 181(13–14):1715–1723
6. Diao W, Tang M, Ding XJ, Zhang Y, Yang JR, Cheng WB, Mo F, Wen B, Xu LL, Yan YR (2016) Electrochemical DNA biosensor based on MNAzyme-mediated signal amplification. Microchim Acta 183(9):2563–2569
7. Ruijter JM, Lorenz P, Tuomi JM, Hecker M, van den Hoff MJ (2014) Fluorescent-increase kinetics of different fluorescent reporters used for qPCR depend on monitoring chemistry, targeted sequence, type of DNA input and PCR efficiency. Mikrochimica Acta 181(13–14):1689–1696
8. Huang S, Lu SY, Huang CS, Sheng JR, Zhang LX, Su W, Xiao Q (2016) An electrochemical biosensor based on single-stranded DNA modified gold electrode for acrylamide determination. Sensor Actuat B-Chem 224:22–30
9. Liu X, Shuai HL, Liu YJ, Huang KJ (2016) An electrochemical biosensor for DNA detection based on tungsten disulfide/multi-walled carbon nanotube composites and hybridization chain reaction amplification. Sensor Actuat B-Chem 235:603–613
10. Rasheed PA, Sandhyarani N (2017) Electrochemical DNA sensors based on the use of gold nanoparticles: a review on recent developments. Microchim Acta 184(4):981–1000
11. Su S, Wu Y, Zhu D, Chao J, Liu X, Wan Y, Su Y, Zuo X, Fan C, Wang L (2016) On-Electrode Synthesis of Shape-Controlled Hierarchical Flower-Like Gold Nanostructures for Efficient Interfacial DNA Assembly and Sensitive Electrochemical Sensing of MicroRNA. Small 12(28):3794–3801
12. Xu ZN, Yin HS, Huo LL, Zhou YL, Ai SY (2014) Electrochemical immunosensor for DNA methyltransferase activity assay based on methyl CpG-binding protein and dual gold nanoparticle conjugate-based signal amplification. Sensor Actuat B-Chem 192:143–149
13. Zhao Y, Zhao JZ, Li YL, Ma DC, Hou SN, Li LZ, Hao XL, Wang ZC (2011) Room temperature synthesis of 2D CuO nanoleaves in aqueous solution. Nanotechnology 22(11):115604
14. Zawisza B, Baranik A, Malicka E, Talik E, Sitko R (2016) Preconcentration of Fe(III), Co(II), Ni(II), Cu(II), Zn(II) and Pb(II) with ethylenediamine-modified graphene oxide. Mikrochimica Acta 183:231–240
15. Yu X, Sheng K, Shi G (2014) A three-dimensional interpenetrating electrode of reduced graphene oxide for selective detection of dopamine. Analyst 139(18):4525–4531
16. Yue HY, Zhang H, Chang J, Gao X, Huang S, Yao LH, Lin XY, Guo EJ (2015) Highly sensitive and selective uric acid biosensor based on a three-dimensional graphene foam/indium tin oxide glass electrode. Anal Biochem 488:22–27
17. Zheng X, Zhu Q, Song H, Zhao X, Yi T, Chen H, Chen X (2015) In situ synthesis of self-assembled three-dimensional graphene-magnetic palladium nanohybrids with dual-enzyme activity through one-pot strategy and its application in glucose probe. ACS Appl Mater Interfaces 7(6):3480–3491
18. Ishikawa R, Bando M, Morimoto Y, Sandhu A (2011) Doping graphene films via chemically mediated charge transfer. Nanoscale Res Lett 6(1):111
19. Lei W, Si WM, Hao QL, Han Z, Zhang YH, Xia MZ (2015) Nitrogen-doped graphene modified electrode for nimodipine sensing. Sensor Actuat B-Chem 212:207–213
20. Zou F, Hu X, Sun Y, Luo W, Xia F, Qie L, Jiang Y, Huang Y (2013) Microwave-Induced in situ synthesis of Zn2GeO4/N-doped graphene nanocomposites and their lithium-storage properties. Chemistry 19(19):6027–6033
21. Yang Z, Cao Y, Li J, Jian Z, Zhang Y, Hu X (2015) Platinum nanoparticles functionalized nitrogen doped graphene platform for sensitive electrochemical glucose biosensing. Anal Chim Acta 871: 35–42
22. Jiang BB, Wei XW, Wu FH, Wu KL, Chen L, Yuan GZ, Dong C, Ye Y (2014) A non-enzymatic hydrogen peroxide sensor based on a glassy carbon electrode modified with cuprous oxide and nitrogen-doped graphene in a nafion matrix. Microchim Acta 181(11–12): 1463–1470
23. Gai PP, Ji YS, Chen Y, Zhu C, Zhang JR, Zhu JJ (2015) A nitrogen-doped graphene/gold nanoparticle/formate dehydrogenase bioanode for high power output membrane-less formic acid/O-2 biofuel cells. Analyst 140(6):1822–1826
24. Feng X, Zhang Y, Zhou J, Li Y, Chen S, Zhang L, Ma Y, Wang L, Yan X (2015) Three-dimensional nitrogen-doped graphene as an ultrasensitive electrochemical sensor for the detection of dopamine. Nano 7(6):2427–2432
25. Rong Q, Feng F, Ma Z (2016) Metal ions doped chitosan-poly(-acrylic acid) nanospheres: Synthesis and their application in simultaneously electrochemical detection of four markers of pancreatic cancer. Biosens Bioelectron 75:148–154
26. Dong W, Wang K, Chen Y, Li W, Ye Y, Jin S (2017) Construction and Characterization of a Chitosan-Immobilized-Enzyme and beta-

Cyclodextrin-Included-Ferrocene-Based Electrochemical Biosensor for H(2)O(2) Detection. Materials (Basel) 10(8):868
27. Yu H, Ye DL, Butburee T, Wang LZ, Dargusch M (2016) Green Synthesis of Porous Three-Dimensional Nitrogen-Doped Graphene Foam for Electrochemical Applications. ACS Appl Mater Interfaces 8(4):2505–2510
28. Cai ZX, Song XH, Chen YY, Wang YR, Chen X (2016) 3D nitrogen-doped graphene aerogel: A low-cost, facile prepared direct electrode for H2O2 sensing. Sensor Actuat B-Chem 222:567–573
29. Guo LQ, Ye PR, Wang J, Fu FF, Wu ZJ (2015) Three-dimensional Fe3O4-graphene macroscopic composites for arsenic and arsenate removal. J Hazard Mater 298:28–35
30. Odeh AA, Al-Douri Y, Voon CH, Mat Ayub R, Subash CB, Odeh RA, Ameri M (2017) A needle-like Cu2CdSnS4 alloy nanostructure-based integrated electrochemical biosensor for detecting the DNA of Dengue serotype 2. Microchim Acta 184(7): 2211–2218
31. Jayakumar K, Rajesh R, Dharuman V, Venkatasan R, Hahn JH, Pandian SK (2012) Gold nano particle decorated graphene core first generation PAMAM dendrimer for label free electrochemical DNA hybridization sensing. Biosens Bioelectron 31(1):406–412
32. Diao W, Tang M, Ding X, Zhang Y, Yang JR, Cheng WB, Mo F, Wen B, Xu LL, Yan YR (2016) Electrochemical DNA biosensor based on MNAzyme-mediated signal amplification. Microchim Acta 183(9):2563–2569
33. Hu YW, Li FH, Han DX, Wu TS, Zhang QX, Niu L, Bao Y (2012) Simple and label-free electrochemical assay for signal-on DNA hybridization directly at undecorated graphene oxide. Anal Chim Acta 753:82–89
34. Peng H-P, Hu Y, Liu P, Deng Y-N, Wang P, Chen W, Liu A-L, Chen Y-Z, Lin X-H (2015) Label-free electrochemical DNA biosensor for rapid detection of mutidrug resistance gene based on Au nanoparticles/toluidine blue–graphene oxide nanocomposites. Sensors Actuators B Chem 207:269–276
35. Sun AL, Zhang YF, Wang XN (2015) Sensitive voltammetric determination of DNA via a target-induced strand-displacement reaction using quantum dot-labeled probe DNA. Microchim Acta 182(7–8):1403–1410
36. Chen Y, Li Y, Yang Y, Wu FN, Cao J, Bai LJ (2017) A polyaniline-reduced graphene oxide nanocomposite as a redox nanoprobe in a voltammetric DNA biosensor for Mycobacterium tuberculosis. Microchim Acta 184(6):1801–1808